A Self-diagnostic Flame Monitoring System Incorporating Acoustic, Optical, and Electrostatic Sensors

Yanchao Zhang
School of Control and Computer Engineering
North China Electric Power University
Beijing, China
120192227037@ncepu.edu.cn

Yong Yan
School of Engineering
University of Kent
Canterbury, Kent CT2 7NT, U. K.
y.yan@kent.ac.uk

Xiaojing Bai
School of Control and Computer Engineering
North China Electric Power University
Beijing, China
baixiaojing@ncepu.edu.cn

Jiali Wu
School of Control and Computer Engineering
North China Electric Power University
Beijing, China
jlwu@ncepu.edu.cn

***Abstract*—Reliable flame monitoring is essential to enhance the safety of industrial boilers. This paper presents a new self-diagnostic system to measure the oscillation frequency of a burner flame. The system incorporates three sensors including a microphone, a photodiode and an electrostatic electrode and simultaneously acquires three signals. The oscillation frequencies from the three sensors are determined through power spectral analysis, and a fused result of the three frequencies is obtained as the oscillation frequency of the burner flame. Moreover, detection and location of the system faults are realized using a self-diagnostic algorithm through the cross-correlation signal processing. Experimental tests were performed on a laboratory-scale combustion test rig with methane as the test fuel. The results demonstrate that the method is capable of measuring the oscillation frequency of a burner flame. In addition, the results are helpful for the comprehensive analysis of the oscillatory behaviors of burner flames. The self-diagnostic algorithm is able to detect the fault of the monitoring system and no additional self-diagnostic hardware is required.**

Keywords—flame monitoring, cross-correlation, oscillation frequency, multi-sensor fusion.

I. INTRODUCTION

The safe operation of an industrial boiler depends on the stable condition of the combustion process. A wide range of fuels is used in power generation, so flames are more complex than before. Sometimes the same power station burns different grades of coal, biomass fuels and even oil. A power plant is operated in a flexible mode so the power output changes frequently. Such flexible operation of a power plant often entails dynamic burner flames. The advanced monitoring of burner flames is desirable for optimized operation of the combustion process.

Earlier monitoring of burner flames was concerned mostly with thermal, optical, thermoacoustic and electrostatic properties. Conventional temperature monitoring devices are dependent upon the prior knowledge of the emissivity of the flame which is usually unknown [1]. Flame monitoring techniques using optical sensors are in line with human's intuitive perception and have been widely used in the power industry [2][3]. However, the measurement results of optical techniques are the luminous superposition perpendicular to the measuring plane, and the optical probe to access the furnace is susceptible to contamination by fine dust and smoke [4]. The energy loss of acoustic signals in a closed chamber is little, because the furnace wall reflects sound waves. Therefore, the acoustic signals represent the combustion process in the whole furnace and are often used for the measurement of thermoacoustic instability [5]. However, the acoustic sources in industrial processes are complex [6][7], and it is unreliable to monitor a flame only using acoustic sensors. Electrostatic sensors have clear advantages including the simplicity in structure, cost-effectiveness and applicability to various environments [8], which are divided into invasive and non-invasive sensors. The former needs to extend a probe into the flame [9], which will inevitably affect the stability and burning rates of the flame, and the electrostatic signals of the latter are closely related to the distance between the flame and the sensor [10]. Every method has its advantages and disadvantages, and the combination of multiple sensors will be a good way of the advanced monitoring of burner flames.

Oscillation frequency of a burner flame indicates its degree of oscillation in luminous intensity, radiation, pressure and concentration of charged species [11]. A variety of flame monitoring techniques have been developed in order to measure the oscillation frequency of a burner flame [12–14]. However, such techniques primarily focus on a single property of the flame and the information is insufficient for monitoring of a complex combustion process. It is desirable to integrate combustion information in different properties to obtain oscillation frequency of a burner flame.

This paper proposes an innovative system incorporating acoustic, optical and electrostatic sensors to monitor the oscillation frequency of burner flames. The oscillation frequency is obtained by fusing the frequency results from three sensing modules. In addition, flame monitors are safety critical devices. If the flame monitor is faulty, then a lot of fuel could be injected to the furnace without the flame, leading to a disastrous outcome for the process operator. Therefore, a self-diagnostic algorithm is proposed to realize the detection and location of the fault module through cross-correlation signal processing. Laminar diffusion flames have the simpler combustion states than turbulent flames and premixed flames, and it is convenient to verify the effectiveness of the monitoring system. Therefore, this paper focuses on the measurement of a laminar diffusion flame. This paper presents the fundamental principle, design and implementation of the

monitoring system. Meanwhile, experimental tests were conducted on a laboratory-scale combustion test rig.

II. Measurement Principle and System Design

A. Sensor Design and Signal Conditioning

The sensing arrangement for the flame monitoring system is shown in Fig. 1. The system includes three parts: a sensing head, a conduit and a signal conditioning box. The sensing head consists of a metal shell, an electrode, a gasket, a printed circuit board (PCB 1) and a lens with a section of optical fibre. The electrode is made of an annular stainless ring and insulated from the metal shell via a quartz gasket. The electrode has an inner diameter of 17 mm and a width of 3 mm. The lens fixed in the middle hole of the gasket is connected with the optical fibre to transmit the optical signal to a photodiode. PCB 1 is designed to embed the microphone and pre-amplify the electrostatic signal. The conduit is hollow so that power and signal cables and the optical fibre are arranged inside for the transmission of signals and power. There are two circuit boards (PCB 2, PCB 3) inside the signal conditioning box. PCB 2, as the main conditioning board, is used to embed the photodiode and complete final signal conditioning. PCB 3 is designed to supply power to the whole system.

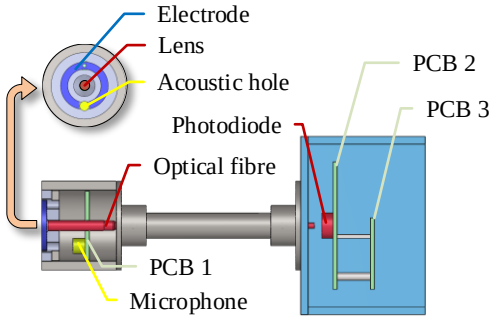

Fig. 1. Schematic illustration of the sensing arrangement.

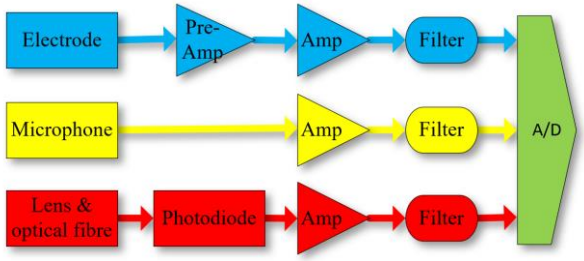

Fig. 2. Block diagram of the signal conditioning process.

Fig. 2 represents the block diagram of the signal conditioning process. The weak electrostatic signal induced by the electrode is amplified by the amplifiers on PCB 1 and PCB 2. The high-frequency noise is filtered out by a low-pass filter on PCB 2. The microphone used is an electret capacitance sensor with a diameter of 6 mm and a height of 2.2 mm. The microphone is connected to the acoustic amplifier and low-pass filter on PCB 2. After passing through the lens and the optical fibre, the optical signal is converted into an electrical signal using the photodiode, and the electrical signal is amplified and filtered on PCB 2. The three sensing modules are independent from each other and their output signals are simultaneously transmitted to the analogue convertor (A/D) for data acquisition.

B. Cross correlation

As the three sensing modules aim at the same flame at the same time, the signals acquired from the modules have a high degree of similarity. Therefore, the evaluation of signal quality can be completed using correlation coefficients between the signals. The correlation coefficient between two signals indicates the degree of their similarity. The normalized version of the cross-correlation function is used to obtain the correlation coefficient [8]:

$$r(m) = \frac{\sum_{k=1}^{N} S_1(k) S_2(k+m)}{\sqrt{\sum_{k=1}^{N} S_1^2(k)} \sqrt{\sum_{k=1}^{N} S_2^2(k)}} \quad (1)$$

where $S_1(k)$ and $S_2(k)$ ($k=1, 2, \ldots N$) are the sampled version of the signals S_1 and S_2, respectively. The magnitude of the dominant peak in the cross-correlation function is the correlation coefficient and ranges between −1 and 1. The greater the correlation coefficient, the more similar the two signals.

If the signal quality is poor or there are faults in a sensing module, the output signal of this module will have a lower level of correlation coefficient with other signals. Based on this point, the correlation coefficient between signals will be used as the evaluating indicator of signal quality in this paper.

C. Oscillation Frequency of Burner Flames

The oscillation frequency of a burner flame is usually derived from the signal through spectral analysis. The oscillation frequency of a laminar diffusion flame is obtained from the power spectrum of a sensor signal in this research, instead of using the peak frequency as the oscillation frequency [9]. The reason is that the multiple sub-peaks often appear near the dominant peak of the power spectrum, and the information in these sub-peaks will be ignored if only the peak frequency is analyzed. The oscillation frequency should reflect the contributions of all components over the entire frequency range. Therefore, a quantitative oscillation frequency (f) is defined as the weighted average frequency over the entire frequency range [15]:

$$f = \frac{\sum_{i=1}^{n} p_i f_i}{\sum_{i=1}^{n} p_i} \quad (2)$$

where f_i is the frequency of *i-th* component, p_i is the power density of the *i-th* frequency component and n is the total number of frequency components.

This paper proposes a new method for the measurement of the oscillation frequency of a burner flame. The correlation coefficients between a signal and the other two signals are used as the weights of data fusion in this research, and the oscillation frequency of a flame (F) is derived based on:

$$F = \frac{(r_{12}+r_{13})f_1 + (r_{12}+r_{23})f_2 + (r_{13}+r_{23})f_3}{2(r_{12}+r_{13}+r_{23})} \quad (3)$$

where r_{12}, r_{13} and r_{23} are the correlation coefficients between the signals from the three sensing modules. f_1, f_2 and f_3 are the oscillation frequencies from the three modules, respectively.

The oscillation frequency in eq. (3) can automatically adjust the weights according to the signal quality, thereby improving the reliability and robustness of the monitoring system.

D. Self-diagnostic Algorithm

When the monitoring system is working normally, the correlation coefficients between the three signals are high due to the similarity of the signals. If a module is abnormal, the output signal of this module will have two low correlation coefficients with other signals. Therefore, low thresholds of correlation coefficients will be selected to detect the faults of the sensing modules. The sensing module with correlation coefficients below the preset threshold is regarded as a faulty module.

In this paper, the acoustic, optical and electrostatic signals are respectively represented by S_1, S_2 and S_3, and R_{12}, R_{13} and R_{23} represents the corresponding thresholds. These thresholds are obtained by analyzing the changes in the correlation coefficients when the module fails. If the three correlation coefficients are all lower than the corresponding thresholds, it means that two or more modules are abnormal. This situation is rare because three modules of the system are of different types and have independent conditioning circuits. If two correlation coefficients are below the corresponding thresholds, such as r_{12} and r_{13}, it means that the S_1 is uncorrelated with the other two signals. And if the other correlation coefficient (r_{23}) is above the corresponding threshold (R_{23}), it means that S_2 and S_3 are correlated and it can be concluded that module 1 is faulty. The possible decisions for the self-diagnosis are listed in Table I. It should be noted that, based on the nature of the cross-correlation function, it is unlikely that only one of the correlation coefficients is below the corresponding threshold. For this reason, the self-diagnostic decision under such conditions is recorded as "–" in Table I.

TABLE I. DECISION FOR FLAME MONITOR SELF-DIAGNOSIS

$r_{12} \leqq R_{12}$	$r_{13} \leqq R_{13}$	$r_{23} \leqq R_{23}$	Self-diagnostic decision
No	No	No	No failure
No	No	Yes	–
No	Yes	No	–
No	Yes	Yes	Module 3 failure
Yes	No	No	–
Yes	No	Yes	Module 2 failure
Yes	Yes	No	Module 1 failure
Yes	Yes	Yes	Multi-module failures

III. EXPERIMENTAL RESULTS AND DISCUSSION

A. Experimental Set-up

To evaluate the performance of the monitoring system, a series of experiments were carried out on a laboratory-scale combustion test rig. As shown in Fig. 3, the test rig consists of a methane gas cylinder, a flow controller, a mass flowmeter, a reference flame monitor, a chamber and a data acquisition system. The flow rates of the methane are controlled with the flow controller and are metered with the flowmeter during the experiments. A Bunsen-type burner with an inner diameter of 24 mm is used to generate laminar diffusion flames in an 80 × 80 × 70 cm^3 chamber which provides a quiescent environment. A mesh screen is mounted across the outlet of the burner to stabilize the flame. The vertical distance between the sensing head and the burner outlet is 30 mm and the horizontal distance is 25 mm. The flame monitoring system is fixed on a supporting frame at the bottom of the combustion chamber. The sensor signals were acquired with a NI USB-6363 data acquisition card (DAQ) at a sampling rate of 5 kHz.

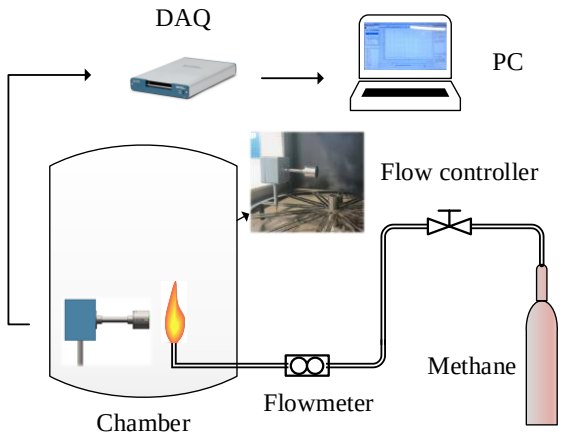

Fig. 3. Constituent elements of the test rig for oscillation frequency measurement.

The experiments consist of two parts: oscillation frequency measurement and fault detection. The former was conducted under seven test conditions with the fuel flow rate over the range of 0.40 L/min to 0.70 L/min at an interval of 0.05 L/min. The latter was conducted at the fuel flow rate of 0.6 L/min. Three types of faults were created, corresponding to the open circuit in each of the three sensing modules.

B. Experimental Results

The time domain waveforms and corresponding power spectra of the signals when the methane flow rate is 0.6 L/min are shown in Fig. 4. The oscillation characteristics of the three signals can be clearly observed. The time domain waveforms exhibit a clear periodicity, and the result reflects the spatial fluctuation characteristics of the flame during the combustion. Due to the characteristic of the photodiode, there are some DC components in the optical signal. This research focuses on the frequency domain characteristics of the burner flames, so the DC component of the optical signal has been filtered out through signal processing. The fluctuation of the acoustic signal is irregular in a single period, which is related to the internal shape of the combustion chamber and the combustion state. It can be noticed that the frequency distributions of the three signals are similar. There are some sub-peaks near the dominant peak for each sensor due to the fluctuation of the combustion state. There are some low-frequency components for the optical signal, which is caused by the geometric fluctuation of the flame [15]. A small number of second harmonics was observed in the power spectra of the acoustic signal, which is related to the thermodynamic fluctuation in the chamber.

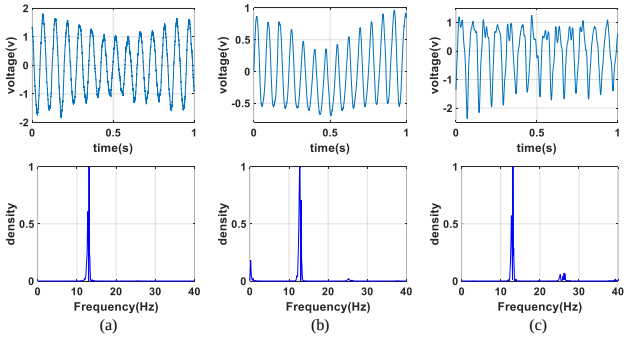

Fig. 4. Time domain waveforms and corresponding power spectra. (a) Electrostatic signals. (b) Optical signals. (c) Acoustic signals.

The oscillation frequency of the diffusion flame for different fuel flow rates is shown in Fig. 5. Each data point is an average of 10 measurements with the standard deviation marked as an error bar. It is evident that the oscillation frequency increases with the fuel flow rate. The measured oscillation frequencies from different sensors are not identical because of the different properties of the burner flame. The acoustic, optical, and electrostatic signals reflect the pressure in the whole chamber, the luminous intensity in combustion zone, and concentration of charged species around the burner flame, respectively. Due to the fluctuations in the combustion conditions, there are some deviations between the frequency results from the repetitive experiments, and the standard deviation is within 0.19 Hz. The fused oscillation frequency reflects the thermoacoustic, optical and electrical properties of the burner flame and is more conducive to the analysis of flame oscillation than that from a single sensor.

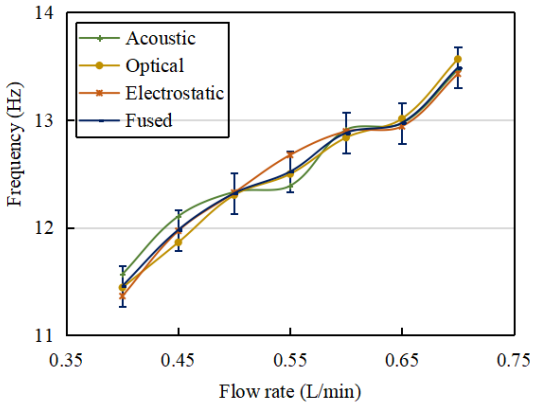

Fig. 5. Oscillation frequency of the diffusion flame for different fuel flow rates.

The typical cross-correlation functions between the signals under normal operation conditions are shown in Fig. 6. All these correlation functions have a clear periodicity and high correlation coefficients. The acoustic, optical and electrostatic signals have different propagation speeds, so the dominant peaks in the cross-correlation functions do not appear at zero time delays.

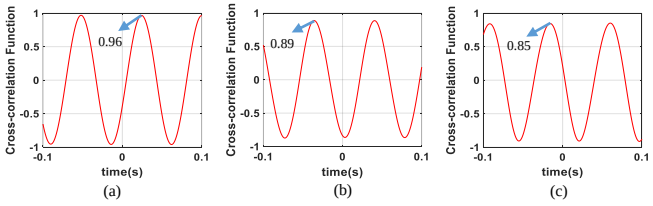

Fig. 6. Typical cross-correlation functions between the signals. (a) Electrostatic and optical signals. (b) Electrostatic and acoustic signals. (c) Optical and acoustic signals.

Correlation coefficients under different faulty conditions are shown in Fig. 7. E-O, E-A, and A-O represent the correlation coefficients between the electrostatic and optical signals, electrostatic and acoustic signals, and acoustic and optical signals, respectively. Under the first (normal) condition the three correlation coefficients are all above 0.8, indicating that each sensing module is working normally. The second condition (E-failure) is that the electrostatic module is faulty. It can be observed that the correlation coefficients between the electrostatic signal and the other two are significantly reduced, and the correlation coefficient between the acoustic and optical signals is still high. The third condition (O-failure) and the fourth condition (A-failure) are similar to the second condition, where the correlation coefficients between the corresponding signal and other two signals reduce significantly and the correlation coefficient between the other signals is still high.

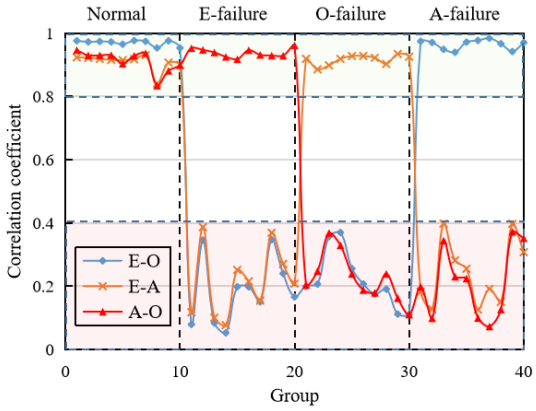

Fig. 7. Correlation coefficients under different faulty conditions.

To realize the self-diagnostic function of the system, the thresholds of the correlation coefficients will be set to detect the fault module. In this study the correlation coefficients are consistently below 0.4 under faulty conditions or above 0.8 during normal operations, so the thresholds of three correlation coefficients (R_{12}, R_{13} and R_{23}) are set to 0.6, which is the average of 0.4 and 0.8. If two correlation coefficients are lower than 0.6 and the third one is over 0.6, the faulty module is identified and the flame monitoring task continues with the other working modules, thereby improving the reliability of the monitor.

IV. Conclusions

This paper has presented a self-diagnostic flame monitoring system incorporating acoustic, optical and electrostatics sensors. A fused oscillation frequency has been determined to describe the oscillation characteristics of burner flames, and a self-diagnostic algorithm has been utilized to realize the detection and location of system faults. The experimental results have shown that this system was able to obtain a comprehensive frequency result based on the optical, acoustic and electrical properties of burner flames. The fault of the system can be detected and located through the self-diagnostic algorithm without additional self-diagnostic hardwares. The overall reliability of the multi-sensing flame monitoring system is better than that of the traditional single-sensing system because it can automatically detect the fault module and continue to work when one sensing module fails. Future work will focus on the evaluation of the system for the measurement of oscillation frequencies of complex flames.

References

[1] E. J. Adamson and R. G. Cumming, “Boiler flame monitoring systems for low NOx applications—An update,” in Pro. Amer. Power Conf., vol. 59, 1997, pp. 340–344.

[2] D. Sun, G. Lu, H. Zhao and Y. Yan, “Flame stability monitoring and characterization through digital imaging and spectral analysis,”Meas. Sci. Technol., vol.22, no. 114007, 2011.

[3] O. F. Moguel, J. Szuhanszki, A. G. Clements, D. B. Ingham, L. Ma and M. Pourkashanian, “Oscillating coal and biomassflames: A spectral and digital imaging approach for air and oxyfuel conditions,” Fuel Process. Technol., vol. 173, pp. 243–252, 2018.

[4] L. Xu and Y. Yan, "A new flame monitor with triple photovoltaic cells," IEEE Trans. Instrum. Meas., vol. 55, no. 4, pp. 1416–1421, 2006.

[5] C. Bhattacharya, S. De, A. Mukhopadhyay, S. Sen and A. Ray, "Detection and classification of lean blow-out and thermoacoustic instability in turbulent combustors," Appl. Therm. Eng., vol. 180, no. 115808, 2020.

[6] J. Ballester and T. Garcia-Armingol, "Diagnostic techniques for the monitoring and control of practical flames," Prog. Energy. Combust. Sci., vol. 36, pp. 375–411, 2010.

[7] A. V. Singh, M. Yu, A. K. Gupta and K. M. Bryden, "Thermo-acoustic behavior of a swirl stabilized diffusion flame with heterogeneous sensors," Appl. Energy, vol. 106, pp. 1–16, 2013.

[8] Y. Yan, Y. Hu, L. Wang, X. Qian, W. Zhang, K. Reda, *et al.* "Electrostatic sensors - Their principles and applications," Measurement, vol. 169, no. 108506, 2021.

[9] Y. Yan, J. Wu and Y. Hu, "Measurement of charge density in methane fired diffusion and premixed flames using electrostatic probes," IEEE Sens. J., vol. 21, pp. 26115–26123, 2021.

[10] J. Wu, Y. Yan, Y. Hu, S. Li and W. Xu, "Flame boundary measurement using an electrostatic sensor array," IEEE Trans. Instrum. Meas., vol. 70, no. 20000412, 2020.

[11] K. R. V. Manikantachari, V. Raghavan and K. Srinivasan, "Effects of burner configurations on the natural oscillation characteristics of laminar jet diffusion flames," Int. J. Spray Combust. Dyn., vol. 7, no. 3, pp. 257–281, 2015.

[12] B. M. Cetegen and T. A. Ahmed, "Experiments on the periodic instability of buoyant plumes and pool fires," Combust Flame, vol. 93, no. 1–2 pp. 157–184, 1993.

[13] X. Jin, Y. Tian, K. Zhao, B. Ma, J. Deng and J. Luo. "Experimental study on supersonic combustion fluctuation using thin-film thermocouple and time–frequency analysis," Acta Astronaut, vol. 179, pp. 33–41, 2021.

[14] Y. Ge, S. Li and X. Wei, "Combustion states distinction of the methane/oxygen laminar co-flow diffusion flame at high pressure," Fuel, vol. 243, pp. 221–229, 2019.

[15] Y. Huang, Y. Yan, G. Lu and A. Reed, "On-line flicker measurement of gaseous flames by image processing and spectral analysis," Meas. Sci. Technol., vol. 10, no, pp. 726, 1999.